

High resolution heterodyne interferometer without detectable periodic nonlinearity

Ki-Nam Joo*, Jonathan D. Ellis, Eric S. Buice, Jo W. Spronck and Robert H. Munnig Schmidt

*Mechatronic System Design, Department of Precision and Microsystems Engineering,
Delft University of Technology, Delft, The Netherlands
k.joo@tudelft.nl

Abstract: A high resolution heterodyne laser interferometer without periodic nonlinearity for linear displacement measurements is described. It uses two spatially separated beams with an offset frequency and an interferometer configuration which has no mixed states to prevent polarization mixing. In this research, a simple interferometer configuration for both retroreflector and plane mirror targets which are both applicable to industrial applications was developed. Experimental results show there is no detectable periodic nonlinearity for both of the retro-reflector interferometer and plane mirror interferometer to the noise level of 20 pm. Additionally, the optical configuration has the benefit of doubling the measurement resolution when compared to its respective traditional counterparts. Because of non-symmetry in the plane mirror interferometer, a differential plane mirror interferometer to reduce the thermal error is also discussed.

©2010 Optical Society of America

OCIS codes: (120.0120) Instrumentation, measurement, and metrology; (120.3180) Interferometry; (120.3940) Metrology.

References and links

1. W. T. Estler, "High-accuracy displacement interferometry in air," *Appl. Opt.* **24**(6), 808–815 (1985).
2. H. Bosse, and G. Wilkening, "Developments at PTB in nanometrology for support of the semiconductor industry," *Meas. Sci. Technol.* **16**(11), 2155–2166 (2005).
3. N. Bobroff, "Recent advances in displacement measuring interferometry," *Meas. Sci. Technol.* **4**(9), 907–926 (1993).
4. F. C. Demarest, "High-resolution, high-speed, low data age uncertainty, heterodyne displacement measuring interferometer electronics," *Meas. Sci. Technol.* **9**(7), 1024–1030 (1998).
5. R. C. Quenelle, "Nonlinearity in interferometer measurements," *Hewlett Packard J.* **34**, 10 (1983).
6. W. Hou, and G. Wilkening, "Investigation and compensation of the nonlinearity of heterodyne interferometers," *Precis. Eng.* **14**(2), 91–98 (1992).
7. S. J. A. G. Cosijns, H. Haitjema, and P. H. J. Schellekens, "Modeling and verifying non-linearities in heterodyne displacement interferometry," *Precis. Eng.* **26**(4), 448–455 (2002).
8. V. G. Badami, and S. R. Patterson, "A frequency domain method for the measurement of nonlinearity in heterodyne interferometry," *Precis. Eng.* **24**(1), 41–49 (2000).
9. T. Eom, T. Choi, K. Lee, H. Choi, and S. Lee, "A simple method for the compensation of the nonlinearity in the heterodyne interferometer," *Meas. Sci. Technol.* **13**(2), 222–225 (2002).
10. H. Haitjema, S. J. A. G. Cosijns, N. J. J. Roset, M. J. Jansen, and P. H. J. Schellekens, "Improving a commercially available heterodyne laser interferometer to sub-nm uncertainty," *Proc. SPIE*, 347–354 (2003).
11. D. Chu, and A. Ray, "Nonlinearity measurement and correction of metrology data from an interferometer system," *Proc. of 4th euspen Int. Conf.*, 300–301 (2004).
12. T. L. Schmitz, D. Chu, and L. Houck III, "First-order periodic error correction: validation for constant and non-constant velocities with variable error magnitudes," *Meas. Sci. Technol.* **17**(12), 3195–3203 (2006).
13. M. Tanaka, T. Yamagami, and K. Nakayama, "Linear interpolation of periodic error in a heterodyne laser interferometer at subnanometer levels (dimension measurement)," *IEEE Trans. Instrum. Meas.* **38**(2), 552–554 (1989).
14. C. M. Wu, J. Lawall, and R. D. Deslattes, "Heterodyne interferometer with subatomic periodic nonlinearity," *Appl. Opt.* **38**(19), 4089–4094 (1999).
15. J. Lawall, and E. Kessler, "Michelson interferometry with 10 pm accuracy," *Rev. Sci. Instrum.* **71**(7), 2669–2676 (2000).
16. T. L. Schmitz, and J. F. Beckwith, "Acousto-optic displacement-measuring interferometer: a new heterodyne interferometer with Angstrom-level periodic error," *J. Mod. Opt.* **49**(13), 2105–2114 (2002).

1. Introduction

Since the Doppler frequency shift measurement technology using a two-frequency source was invented in the 1970s, heterodyne laser interferometry has been widely used as an accurate positioning sensor to measure displacements of precision stages [1]. The heterodyne laser interferometer has also been widely used to calibrate other measurement tools such as capacitive sensors, inductive sensors, and optical encoders because of its high dynamic range, high signal-to-noise ratio, and direct traceability to the length standards [2]. Subnanometer level measurements must be achieved to satisfy industrial demands on performance [3]. The rapid development of electronic phase measuring technology made it possible to measure subnanometer displacements in combination with optical resolution determined by interferometer configurations. When a HeNe laser ($\lambda=632.8$ nm) is used as an optical source, a commercial displacement interferometer with retro-reflectors, which has the optical resolution of $\lambda/2$ (316.4 nm), can achieve displacement measurements with a $\lambda/2048$ (0.31 nm) resolution from fringe interpolation [4]. The phase measuring electronics, however, introduce a measurement error caused by periodic nonlinearities in the interferometer which deteriorates the purity of the interference signals [3].

From previous research [5–7], it is clear the periodic nonlinearity originates from a mixed heterodyne source and non-perfect polarizing optics. Because a two frequency, orthogonally polarized source is used, there will be non-orthogonality errors and slightly elliptical beams which contribute errors. These combined with imperfect polarizing optics, polarization alignment between the source and optics, ghost reflections, and electronic nonlinearity all created additional nonlinearity errors [3]. Small leakage components from these invoke an unexpected phase change between reference and measurement signals. When the geometrical errors are minimized, periodic nonlinearity is the fundamental error source limiting the implementation of subnanometer displacement measurements. This assumes the measurement is performed in an ideal environment, such as in vacuum, or when the measurement length minimized so the refractive index effects are minimal.

Reducing errors from periodic nonlinearity has been the subject of much research, which can be categorized as either algorithm methods [8–12] or two spatially separated beam interferometer configurations [13–17]. The reduction method algorithms ensure a periodic nonlinearity below 1 nm without changes to the interferometer configuration; however, they require the calibration and additional calculation time. On the other hand, real time reductions can be implemented with modified interferometer setups using two spatially separated beams. The only limitation of these interferometer configurations is their special and often complicated configurations which limit their applicability in industrial and scientific fields.

In this research, we describe two simple heterodyne interferometer configurations, with a retroreflector and with a plane mirror, with two spatially separated beams to eliminate the periodic nonlinearity. These interferometers have a minimum number of optical components and the opposite phase shift direction between interference signals enhances the optical resolution by a factor of two. This optical resolution enhancement allows for simpler optical configurations while achieving the same optical resolution by increasing the number of beam paths in the interferometer.

2. Simple retroreflector interferometer without periodic nonlinearities

Figure 1 shows the heterodyne laser source and retro-reflector interferometer configuration. Because the periodic nonlinearity initially comes from the heterodyne laser source, which has polarization and frequency mixing, two acousto-optic frequency shifters (AOFS₁, AOFS₂) to generate two different frequencies, ($f_0+\delta f_1$) and ($f_0+\delta f_2$), from a stabilized single frequency (f_0) source were used. By doing so, a beat frequency of ($\delta f_2-\delta f_1$) is created and each beam has no leakage component to cause periodic nonlinearities [14]. The original beams with f_0 from AOFS₁ and AOFS₂ were blocked with pinholes (PH), which were approximately 200 mm

apart from the AOFSs. These two beams from the source part were adjusted and aligned with three mirrors to ensure two separated, parallel beams before entering the interferometer as illustrated in Fig. 1.

The interferometer, as depicted in the upper portion of Fig. 1, consists of a beam splitter (BS_2), a right angle prism (RAP) as the reference mirror, and a retro-reflector (RR) as the moving target. As shown in Fig. 1, two parallel beams, where the solid and dotted line indicating top and bottom beams, respectively, travel to BS_2 . The reflected beam travels toward the RAP, which has line symmetry. The transmitted beam travels to the RR, which has point symmetry [17]. When both the reference and measurement beams hit their respective targets, they will change vertical position, i.e. the bottom beam will go to top and vice versa, which allows for the reference and measurement beams to recombine at BS_2 to create interference with opposite phase directions, detected by the photodetectors (PD_R and PD_M). From the PD_R and PD_M , the phase difference $\varphi=8\pi\Delta L/\lambda$ (where ΔL is the displacement of the RR and λ is the wavelength of light), which results in an optical resolution of $\lambda/4$, can be obtained. The main advantage of this interferometer is there is no possibility to generate any leakage beams in the optics, which means periodic nonlinearities are essentially eliminated. Moreover, the optical resolution is doubled without a complicated beam path because the phase direction between two interference signals is opposite. This interferometer was optimized to have minimum optical components as well as no expensive custom optics, so it can be easily applied to industrial and science fields.

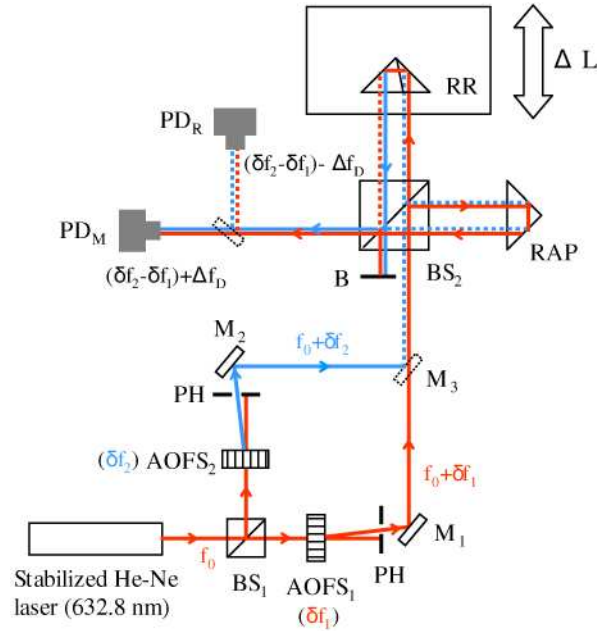


Fig. 1. The optical configuration of a high resolution heterodyne laser interferometer with no detectable periodic nonlinearity; BS_1 , BS_2 , beams splitters; $AOFS_1$, $AOFS_2$, acousto-optic frequency shifters; PH, pinhole; M_1 , M_2 , M_3 , adjustable mirrors; RR, retro-reflector; RAP, right angle prism; B, beam blocker; PD_R , PD_M , reference and measurement photodetectors, respectively. The dotted line is used to indicate that the beam is at the bottom. Δf_D is the Doppler shift from the stage motion (ΔL).

While the spatially separated source is somewhat complicated, this could be remotely located and the beams could be directed to the interferometer using optical fibers, which is done in most precision industrial applications. This removes a heat source from the interferometer. The frequency stability of the three mode HeNe laser, used as a stabilized source in our research, was on the order of 10^{-10} . The central mode provided approximately 2 mW of power, which is much higher than typical commercial sources. After splitting and

frequency shifting, there was approximately 0.75 mW of power per beam (~1.5 mW total), depending on alignment, which can be split for multi-axis systems without significant power loss.

Figure 2 shows the measured wrapped phase of the interferometer compared to a typical heterodyne laser interferometer with a Zeeman split frequency laser (632.8 nm). The phase was measured by a custom built phase meter in a dSPACE data acquisition system, while the retro-reflector in Fig. 1 was translated using a piezoelectric-driven stage (MAX311, Thorlabs). The positioning stage was operated in closed loop and controlled with approximately 20 nm steps. As shown in Fig. 2, the wrapped phase measured in the proposed interferometer is twice as fast as the typical interferometer according to the stage motion. It is noted that the 20 nm step motion was averaged with the low pass filter to simply compare the wrapped phases in Fig. 2. This observation confirms that the optical resolution is improved by a factor of two.

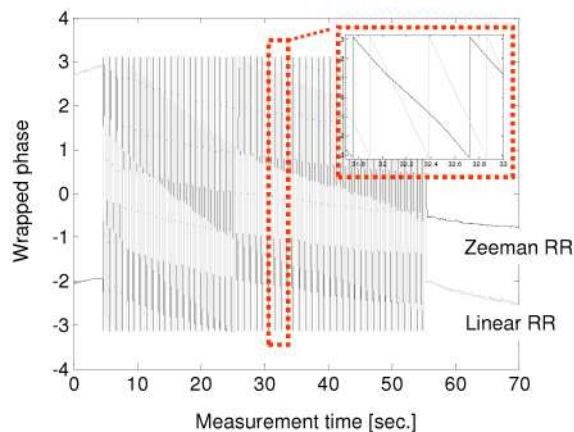


Fig. 2. Measured wrapped phase of the interferometer depicted in Fig. 1 (Linear RR, grey line) and a typical interferometer (Zeeman RR, black line). In both interferometer configurations a retro-reflector is used as a measurement target. The inset means the phase change of our interferometer is twice as faster as that of the typical one.

To evaluate the periodic nonlinearity, the measured displacements were fitted with a low order polynomial to remove the large nonlinear motions of the stage. The residual difference between the measured and fitted data was applied to a fast Fourier transform (FFT) to detect the periodicity [15]. To reduce the noise from undesired stage vibrations, the FFT results of 10 measurements were averaged. Since the nonlinearity shows up as a periodic measurement, the FFT results plotted against the nominal fringe frequency can be used to determine the error based on the fringe order. Figure 3 presents a periodic nonlinearity comparison of the two interferometers according to the fringe order in the FFT domain. It should be noted this method assumes the periodic stage motion errors and mount vibration errors do not occur at the same frequency as the first and second order optical errors.

The periodicity for the typical interferometer using a Zeeman laser was determined to be approximately 7 nm at the first fringe order, as shown in Fig. 3(a). While no periodic nonlinearity is detectable with the proposed interferometer at half, first and second fringe order, several peaks appeared in the Fig. 3(b) however. Those peaks are caused by the residual vibration effects from the stage motion after averaging and resolution limitations of the phase measuring electronics. The peaks appeared apart from the fringe orders while the periodic nonlinearity was below the noise level of approximately 20 pm. The noise level was caused from the electronic measuring board, shot noise of the detectors, and mechanical vibrations, and minimizing these effects is needed to improve the accuracy of this system.

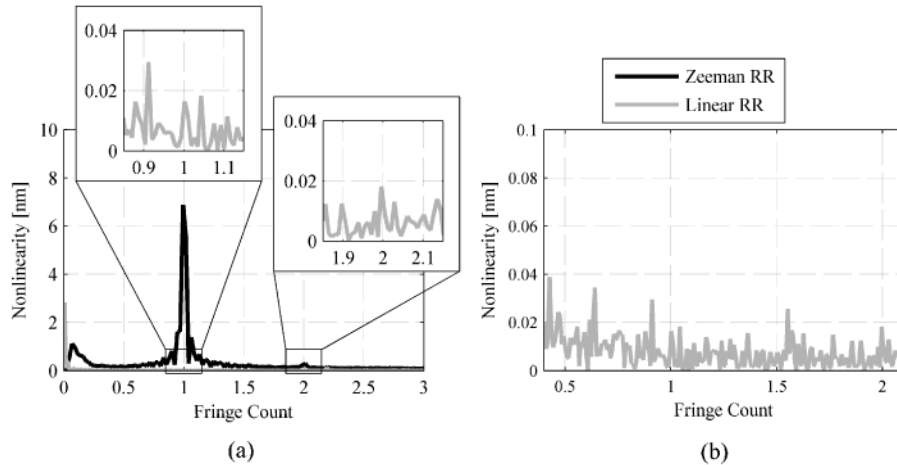


Fig. 3. (a) FFT analysis of the difference between measured displacements and the fitted one in our interferometer (Linear RR, grey line) and the typical interferometer (Zeeman RR, black line), (b) enlargement of the FFT results in the proposed interferometer. The periodic nonlinearity of approximately 7 nm was detected in the typical interferometer while there was no observable periodic nonlinearity in the proposed interferometer except for peaks caused by vibrations.

3. High resolution plane mirror interferometer

The interferometer concept to separate the two beams and use a right angle prism can also be adapted for plane mirror targets, as shown in Fig. 4, which are commonly used in multi-degree of freedom systems. Instead of a retro-reflector target, a plane mirror interferometer (PMI) which consists of a polarizing beam splitter (PBS), a quarter-wave plate (QWP), a retro-reflector (RR) and a flat mirror (M) are included in the basic configuration. In this interferometer, the optical resolution becomes $\lambda/8$ (79 nm) because of the double-path interferometer setup. The reference and measurement beams are completely separated until they are recombined by the BS, which eliminates the chances for frequency or polarization mixing. With the exception of ghost reflections, there is also no beam leakage present, thus it is theoretically free from periodic errors. Figure 5 shows the FFT analysis of the experimental displacement results compared to a commercial 2-pass plane mirror interferometer (E1826G, Agilent). Similar to the retro-reflector interferometer case, the wrapped phase was twice faster and no periodic nonlinearity was detected, while the commercial interferometer has the first order nonlinearity of approximately 0.3 nm, as shown in Fig. 5(a). Although several peaks appeared in the FFT domain, these peaks originate from the stage motion vibrations. Because of the optical resolution doubling, these vibration peaks shift to half the original frequency between the Agilent PMI measurements and our Linear PMI measurements. The three peak pairs are shown in Fig. 5(b), where the fringe order is halved between the two measurements but the amplitude is approximately the same.

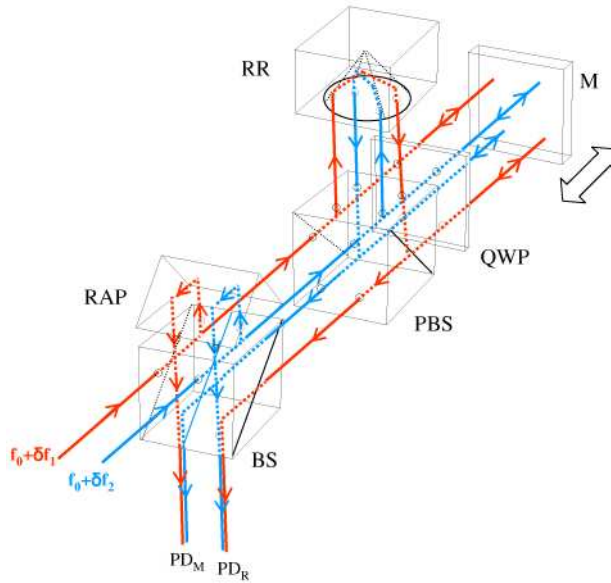


Fig. 4. The schematic of plane mirror interferometer with two spatially separated beams and right angle prism; BS, beams splitter; PBS, polarizing beam splitter; QWP, quarter-wave plate; RR, retro-reflector; RAP, right angle prism; M, target mirror; PD_R, PD_M, reference and measurement photodetectors, respectively.

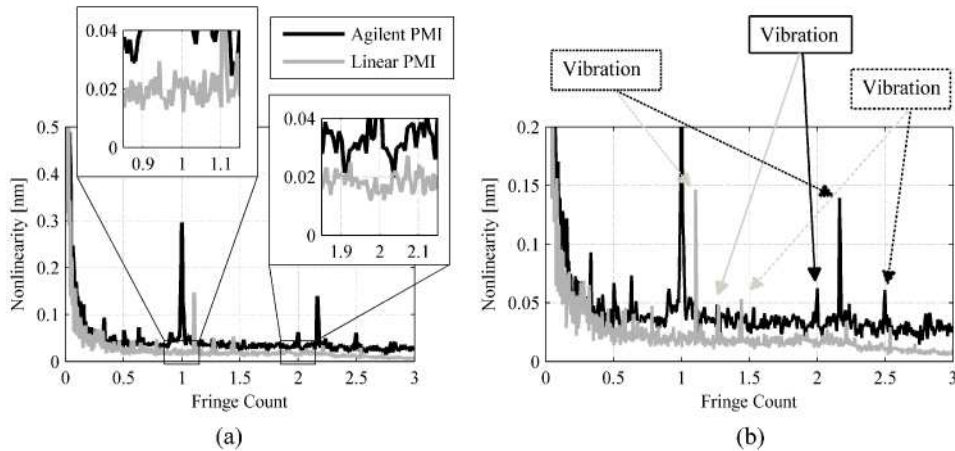


Fig. 5. (a) FFT analysis of the difference between measured displacements and the fitted one in the proposed interferometer (Linear PMI, grey line) and the commercial interferometer (Agilent PMI, black line), (b) indicating several peaks caused by stage vibrations in both of the results. The peaks of the commercial interferometer were matched with the peaks of our interferometer considering the optical resolution.

4. Discussion

The drawback of the linear plane mirror interferometer in Section 3 is that the configuration is unbalanced between the reference and measurement paths. Due to the additional path of the measurement beam in the optical components such as a PBS and a QWP, temperature fluctuations can give rise to the significant thermal errors in the interferometer. To avoid or minimize these thermal errors, a differential type plane mirror interferometer was considered

in this research. Figure 6 shows the proposed plane mirror interferometer which has the differential path between the reference and measurement mirrors. Although this interferometer is not perfectly balanced, the configuration is nearly balanced, so the thermal effects on the optical components can be reduced.

The two parallel beams are divided by a linear displacement beam splitter (DBS) into two sets, reference beams and measurement beams. Similar to a typical plane mirror interferometer, each set of beams has the double-path between a PBS and mirrors. The measurement beams are reflected by a RR experiencing the point symmetry while the reference beams have the line symmetry with a RAP. The two sets of beams propagate back to the DBS and are then recombined to make the heterodyne signals. The heterodyne signals from photodetectors, PD_R and PD_M , again have phase changes in the opposite directions induced by the Doppler shift and are used for reference signal and measurement signal respectively. In this interferometer, the optical resolution is also $\lambda/8$ because of the double-path interferometer setup.

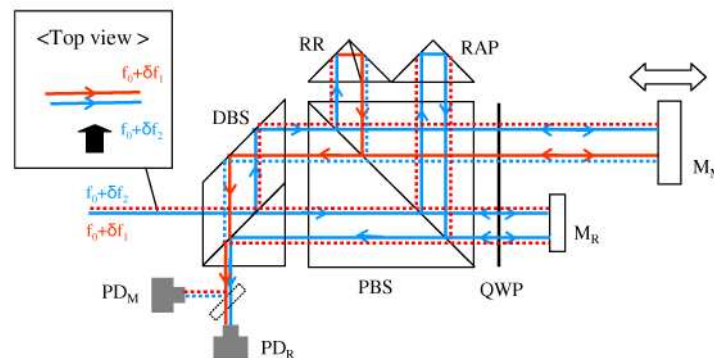


Fig. 6. The differential plane mirror interferometer configuration; DBS, displacement beams splitter; PBS, polarizing beam splitter; QWP, quarter-wave plate; RR, retro-reflector; RAP, right angle prism; M_R , M_M , reference and measurement mirrors; PD_R , PD_M , reference and measurement photodetectors, respectively. The dotted line is used to indicate that the beam is at the bottom.

5. Conclusion

In this paper, a heterodyne laser interferometer with no detectable periodic nonlinearity was proposed and verified. This interferometer used two spatially separated beams to prevent any source mixing and polarization leakage. Moreover, the optical resolution was enhanced by a factor of two due to the opposite phase change direction between reference and measurement signals. To verify our interferometer, a retro-reflector and plane mirror interferometer configurations were tested and compared with typical interferometers. The optical resolution enhancement was confirmed and the periodic nonlinearity was below the measurement noise level, which was approximately 20 pm.

This work was supported by the Dutch IOP (projects IPT06104 and IPT04001) in the Netherlands. The authors would like to acknowledge Agilent Technologies and VSL Dutch Metrology Institute for their equipment support.